

## NUMERICAL MODEL AND EXPERIMENT TO DETERMINE STRESS AND DISPLACEMENT OF STEEL BOX GIRDER BRIDGE STRUCTURE

### NUMERIČKI MODEL I EKSPERIMENTALNO ODREĐIVANJE NAPONA I POMERANJA ČELIČNOG KUTIJASTOG NOSAČA KONSTRUKCIJE MOSTA

Originalni naučni rad / Original scientific paper

Rad primljen / Paper received: 28.04.2025

<https://doi.org/10.69644/ivk-2025-03-0501>

Adresa autora / Author's address:

<sup>1)</sup> University of Transport Technology, Hanoi, Vietnam  
B.T. Phung <https://orcid.org/0009-0003-5796-3465>

<sup>2)</sup> Le Quy Don Technical University, Hanoi, Vietnam

T.C. Nguyen <https://orcid.org/0000-0001-9723-5161>

\*email: [trongchuc.nguyen@lqdtu.edu.vn](mailto:trongchuc.nguyen@lqdtu.edu.vn)

<sup>3)</sup> University of Transport and Communications, Hanoi, Vietnam

H.H. Nguyen <https://orcid.org/0009-0007-0564-2159>

#### Keywords

- steel box girders
- warping section
- stress
- displacement
- numerical model
- experiment

#### Ključne reči

- čelični kutijasti nosači
- vitoperenje poprečnog preseka
- napon
- pomeranje
- numerički model
- eksperiment

#### Abstract

The need to develop the city's transportation system is growing in tandem with the development of society. Congestion in urban areas is a difficult problem that has been and continues to be addressed. Building overpass systems at intersections is one way to quickly solve that problem. Because of the shorter construction time, steel overpasses are more convenient in the city than pre-reinforced concrete overpasses. Therefore, steel box girders have been widely used for straight and curved highway and transit structures over the last decade. To meet the demand for such structural elements, design criteria had to be developed. Despite the fact that many steel bridges have been built, there have been few studies on how this structure works, particularly the warping effect in the steel beam section. The study presents modelling and experiments to determine the stress and displacement of a steel box bridge structure taking into account the section warping effect. Results demonstrate that when the plate element model is used to model, the results are reliable. Research findings will be used as a reference for steel box girder bridge structure design projects in Vietnam.

#### Izvod

Potreba za razvojem gradskog saobraćajnog sistema raste u tandemu sa razvojem društva. Prenaseljenost u urbanim sredinama je veliki problem koji se spominjao i nastavlja da se spominje. Izgradnja sistema pešačkih mostova preko raskrsnica je jedan od načina kojim se brzo rešava problem. Zbog kraćeg vremena izgradnje, čelični mostići su pogodniji u gradu u odnosu na mostiće od prednapregnutog betona. Stoga se čelični kutijasti nosači uveliko koriste za prave i krivolinijske konstrukcije na autoputevima i obilaznicama tokom proteklih desetak godina. Razvijeni su kriterijumi projektovanja kako bi se ostvarili zahtevi za ovakvim konstrukcionim elementima. Uprkos činjenici da je izgrađeno mnogo čeličnih mostova, postoji mali broj studija o funkcionalnosti ovakvih konstrukcija, posebno efekat vitoperenja preseka čeličnog nosača. U radu su opisani modeliranje i eksperimenti za određivanje napona i pomeranja čelične konstrukcije nosača mosta, uzimanjem u obzir vitoperenje preseka. Pokazuje se da su rezultati pouzdani korišćenjem modela pločastog elementa. Dobijeni rezultati će se upotrebiti kao referenca za projektovanje čeličnih kutijastih nosača mostnih konstrukcija u Vijetnamu.

#### INTRODUCTION

The need to improve the city's transportation system is growing along with society's development. Traffic congestion is a challenging issue that has been and is still being addressed in urban areas. Building overpass systems at intersections is one way to solve that issue quickly. Due to their quick construction, steel overpasses are more practical to build in cities than pre-reinforced concrete overpasses /1-3/.

Although there are many steel bridges in Hanoi and Ho Chi Minh City in Vietnam, there are still very few domestic studies on how these kinds of structures function, particularly their effectiveness, and response to warping in the cross-section of steel beams. The I-section and box-section are two primary cross-sections of steel bridges. When used

on curved bridges, intersections are bridges with a lot of torque, and the steel box girder bridge has the advantage of torsion stiffness. A steel box girder bridge cross-section can take the shape of a single box (Fig. 1a), several individual boxes (Fig. 1b), or a box with multiple partitions (Fig. 1c), depending on the width of the deck /3/.

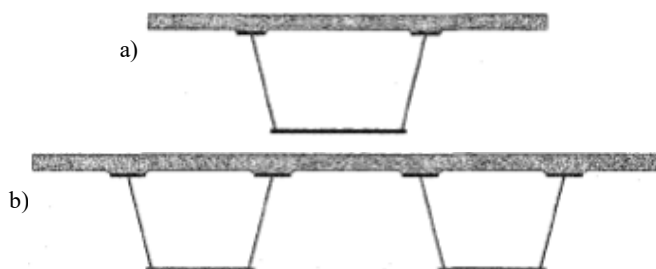




Figure 1. Typical cross-sections of steel box girder bridges /3/.

Steel bridges usually have two types including bridge decks, reinforced concrete slabs combined with steel beams and orthogonal slab decks. The reinforced concrete slab deck is combined with the steel beams by means of shear studs (shear stud) (Fig. 3). Steel orthogonal slab structures are used for large bridges to reduce deck static load and conserve materials. The orthogonal slab serves as both the deck slab and a main girder component. The upper longitudinal connection system can be removed because the orthogonal plate connects the main beam branches (Fig. 2) /4/.

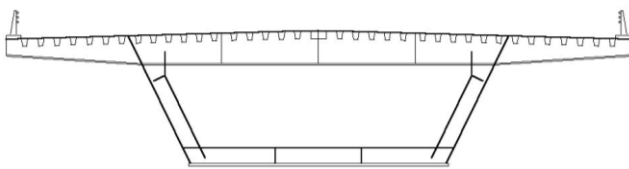


Figure 2. Box girder bridge with orthogonal slab structure.

Basic parts of a composite steel box girder bridge shown in cross section include: bottom slab (bottom flange), web, top flange and reinforced concrete deck (concrete deck), closed box-shaped cross-section of the bridge. Anchor connection (shear stud) to ensure the union between steel beam and reinforced concrete slab, against the sliding force and separation between the steel beam and reinforced concrete slab /4/.

The vertical connection system and the horizontal connection system are both parts of the box girder bridge's connection system. The internal bracing system is depicted as a K-frame in Fig. 3a. The box girder warping deformation is controlled by the connection system. The shape of this K-frame connection system makes it simple to travel inside the box during construction or inspection during use. To control torsion during construction and erection, the upper wing of the beam should have the truss form shown in Fig. 3b, /4/.

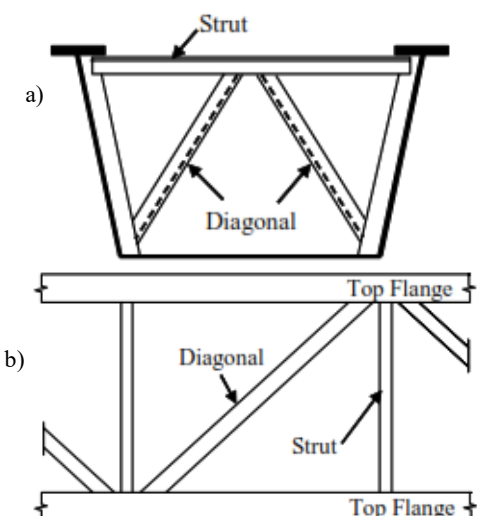


Figure 3. Typical connection system in steel box girder bridge, /4, 5/.

Figure 4 shows a two-box girder using a K-shaped external brace at intermediate points along bridge length. The effect of these K braces is to control the relative torsion between adjacent boxes, distributing internal forces. However, due to fatigue, these braces will be removed after the bridge is completed. In addition to K-type braces, X-bracing frames can be used (Fig. 5).



Figure 4. External connection system between box girders, /4, 5/.

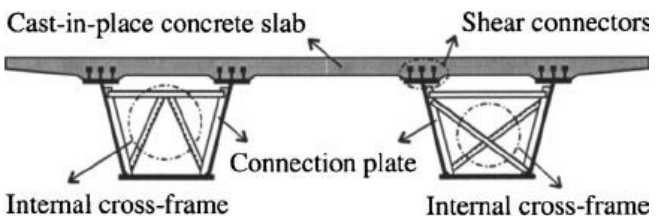


Figure 5. Cross-linking system of K- and X-frame braces.

The combined steel box girder solution satisfies the aforementioned criteria with exceptional benefits in span, high torsional stiffness, high aesthetics, durability, and good maintainability. The steel box girder is better for longer spans than the I-beam because it has higher flexural strength. The actual span is roughly 45-100 m. This structure's span is 160 m (Kanawha River bridge in Virginia, USA). Because the steel box girder structural form is more intricate than the I-beam, manufacture and installation of one calls for highly skilled labour. Additionally, the weight of each steel box girder unit is typically higher than that of an I-beam, increasing the cost of construction. However, when compared to the I-beam span system, the steel box girder span system uses fewer main girders, transverse beams, and bracing systems, which lowers manufacturing costs as well as site labour costs. The characteristic of this type of beam is its high torsional rigidity, so it is very suitable for curved bridges in intersections and ramps. Two bridges built in the US have a very small curvature of 45 m (in Massachusetts, 1960) and 55 m (airport jetty at Dallas, 1970). In contrast to other types of bridges, however, it should be noted that manufacturing vertical, horizontal, extremely high, and diagonal bridges can be challenging. Aesthetics is a notable benefit of steel box girder bridges. The bracing system, reinforcing ribs, utilities, and other components are 'hidden' in the box, not being exposed and causing 'distractions,' while minimising the risk of dust and dirt. This is in contrast to the integrated I-beam bridge. The direct corrosive effects of the environment are because they are 'protected' inside the box, which lowers the cost of the coating system and makes it easy to conduct inspection and maintenance work inside the box, /2/.

## SUBJECTS AND RESEARCH METHODS

## Research subjects

Construction site: the overpass at O Dong Mac - Nguyen Khoai intersection is built to limit traffic jams at the intersection of Tran Khat Chan - Nguyen Khoai streets with Lo Duc-Kim Nguu street, Hanoi city, Vietnam.

Bridge characteristics: the bridge is permanently designed with steel box girders combined with reinforced concrete slabs.

Design standard: TCVN 11823-2017 /6/.

Dimensions of cross section:  $B = 2 \times 3.5 + 2 \times 2 + 2 \times 0.5 = 12$  m.

Static without traffic:  $H = 4.75$  m.

Design speed:  $V_{dk} = 40$  km/h.

Bridge span diagram: 45 + 56 + 72 + 56 m.

Total length of bridge to rear of the abutment:  $L_{tc} = 232.4$  m.

The bridge structure is a composite steel box girder with continuous reinforced concrete deck slab with span length 45 + 56 + 72 + 56 m. The cross section is in the form of a steel box girder with reinforced concrete deck slab of height at the top of the main pillar  $h = 2.11$  m, in the middle of the span  $h = 1.05$  m.

## Working characteristics of steel box girder bridge

Consider the load in the cross-section of the eccentrically box-shaped steel box girder,  $P$ , which is analysed into bending and torsion components, Fig. 6.

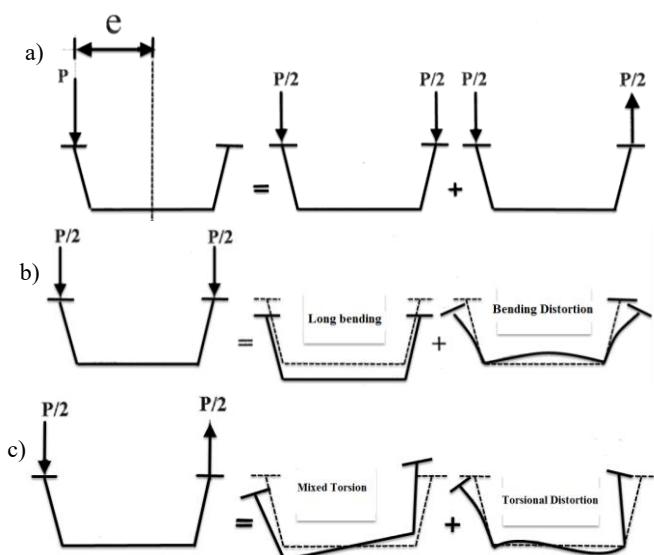


Figure 6. Analysis of load components  $P$  in open box girders according to the co-operative principle: a) loading components; b) bending load actions; c) torsional load actions /5, 7/.

Bending loads can warp and buckle sections (Fig. 6b). When impact loads are applied to beams, a common phenomenon known as longitudinal bending takes place. The cross-section is frequently assumed to always be flat when performing the calculation. When loads are applied to open boxes, deformation occurs. This distortion leads to bending in ribs, lower flange, and upper flange of open box girders (Fig. 6b). The cross-sectional shape of the slabs is altered by the out-of-plane bending of the beams that make up the slabs. For this reason, investigating the displacement of points on the cross-section will produce conclusive findings about the phenomenon.

Torsional load is induced on the section (Fig. 6c). Due to the curvature of the bridge, lateral loads acting on a box girder cause torsion about girder's longitudinal axis. The cross-section is frequently assumed to always be flat when performing the calculation. Steel plates are bent and their cross-sections are deformed by torsion. In order to clearly see the effects of this phenomenon, one should study the displacement of points on the cross-section.

## Theoretical methods to determine the stress-strain state of steel box girders

Theory of torsion: in thin-walled sections as box girders, shear stresses generate torque, leading to two main types of twisting: Saint-Venant torsion and warping torsion. Saint-Venant torsion results from shear deformation, while warping torsion arises from bending within plate planes /8/. Though both occur in box girders, Saint-Venant torsion generally provides most of the torsional stiffness and often allows to neglect stresses from warping. Box girders can be 100-1000 times stiffer in torsion than I-beams, with stiffness depending on the material shear modulus  $G$  and torsion constant  $K_T$  /9/.

$$M_T = G K_T \frac{d\phi}{dx}, \quad (1)$$

where:  $M_T$  is torque of the components on the cross section;  $G$  is shear modulus of elasticity;  $\phi$  is rotation angle of the cross section;  $x$  is vertical axis of the element.

The torsional constant of the beam of a thin-walled box is determined by the expression, /10/:

$$K_T = \frac{4 A_0^2}{\sum_i b_i / t_i}. \quad (2)$$

Here,  $A_0$  is the closed cross-sectional area of the box girder;  $b_i, t_i$  are the width and thickness of the  $i$ -th panel of the box, respectively.

Saint-Venant torsional shear stress can be used using Prandtl's membrane analogy /11, 12/. For example, for a single-box beam, the uniform shear stress  $q$  along the perimeter of the box can be determined by Bredt's equation:

$$q = \tau t = \frac{M_T}{2 A_0}, \quad (3)$$

where:  $t$  is thickness of plate;  $\tau$  is constant stress along the thickness of plate. The torsion stress distribution is shown in Fig. 7.

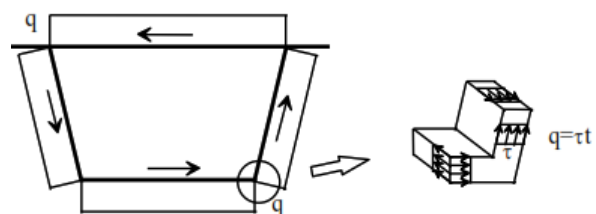


Figure 7. Sliding deformation in box girder caused by Saint Venant torsion.

In box girders, torsional warping stresses are often neglected, but distortion under load can still induce significant warping. Although torque can be applied without changing the cross-section shape, real-world factors as eccentric loading and bridge geometry often lead to deformation. This dis-

tortion causes warping in individual plates of the girder, producing longitudinal stresses due to out-of-plane bending /13/. These warping stresses depend on girder geometry and the intensity of the applied load.

#### Theoretical method of orthogonal slabs to determine the stress state of steel box girders

Steel box girder bridges can be analysed using various methods that simplify the complex spatial structure through assumptions about geometry, materials, and connections. The accuracy of these analyses depends heavily on the chosen assumptions and techniques /14, 15/.

The orthogonal slab method accounts for the interaction between the concrete slab and steel box girder by distributing the transverse beam's stiffness across an equivalent orthogonal plate. While useful, this method faces challenges in accurately estimating bending and torsional stiffness, as well as stress distribution in slabs and beams /16, 17/.

#### Numerical method for determining the stress and strain states of steel box girders.

The finite element method (FEM) is the most widely used numerical technique for solving complex engineering problems efficiently and accurately. It works by dividing a structure into small elements connected by nodes and applying

boundary and continuity conditions. Structural unknowns, such as deformation and displacement at the nodes, are determined using mechanical principles like energy or virtual displacement principle. FEM is commonly implemented in software such as Midas, RM, SAP, Ansys, and Abaqus, which are widely used in bridge design. The method employs both one-dimensional elements (beams, bars) and two-dimensional elements (plates, shells, solids) /18-20/.

The finite element method is considered a modern and comprehensive tool widely adopted in structural analysis due to its ability to efficiently solve large-scale, complex problems. However, when using bar elements with six degrees of freedom per node, it may not accurately capture warping and distortion effects in curved steel box girders. These limitations make it necessary to perform a more detailed analysis using plate elements, which better reflect the true behaviour of the structure and align with the stress calculation methods discussed.

## RESULTS AND DISCUSSION

### Experimental model

Figure 8 depicts the tenso mounting position for measuring stress and displacement mounted on a steel box girder structure.

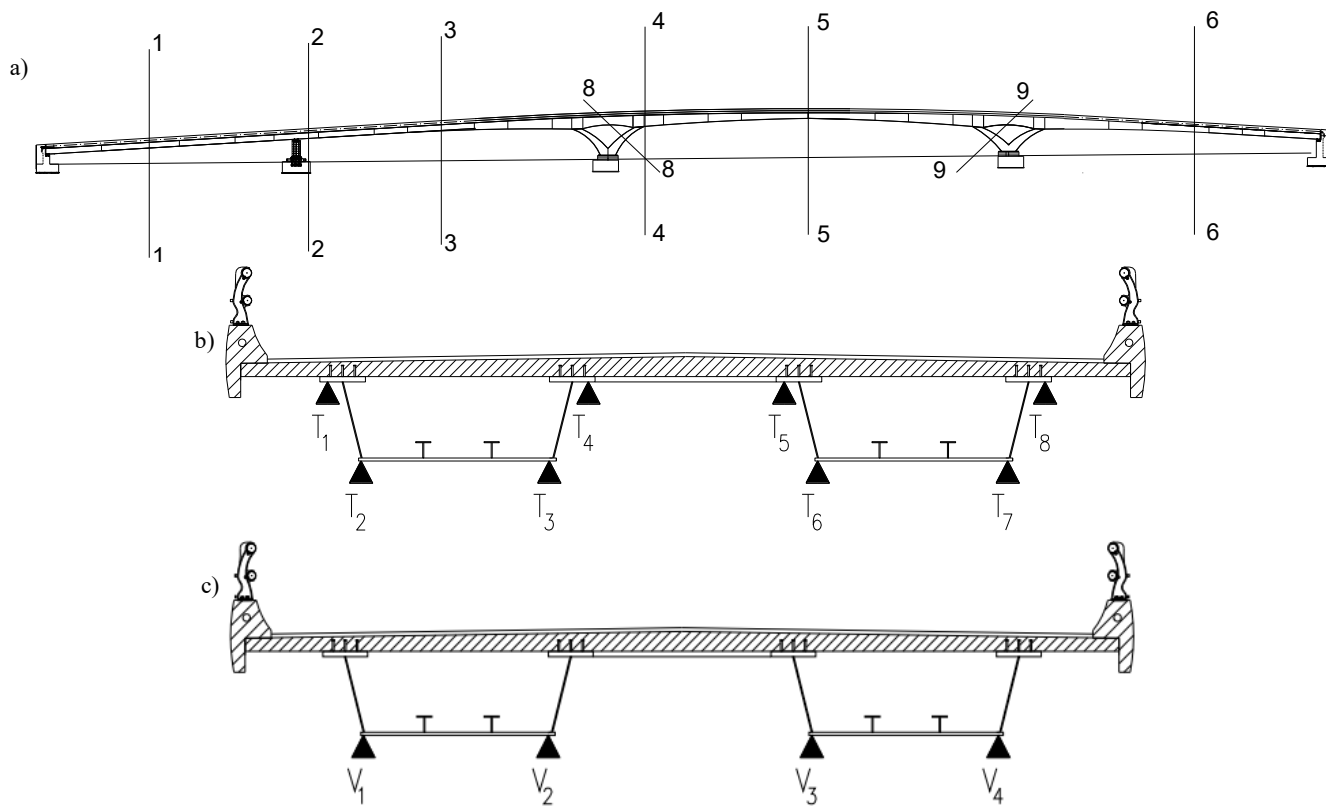


Figure 8. Arrangement of measuring points for stress and displacement of main span main girder: a) 1-1 is the cross-section measuring the stress and displacement of main span main girder; b) arrangement of measuring points on the bridge cross-section; c) arrangement of displacement measurement points.

### Test load

The effect brought about by the test load is at least 70 % of the effect brought about by the design vehicle load taking the shock into account.

$$0.7(1+\mu)S \leq S_{try}, \quad (4)$$

where:  $S_{try}$ ,  $S$  are effect of test load and the effect of design load of the bridge or the design load according to the information from the management.

The load used for the load test includes 9 3-axle unibody vehicles with the following parameters:

Distance from front axle to middle axle of vehicle *a*: 3.0 - 3.8 m;  
 Distance from middle axle to rear axle of vehicle *b*: 1.2 - 1.4 m;  
 Distance between centre of the two wheels in the horizontal direction of the bridge: 1.8 - 1.9 m;  
 Vehicle weight (including vehicle weight): 13-15 T.

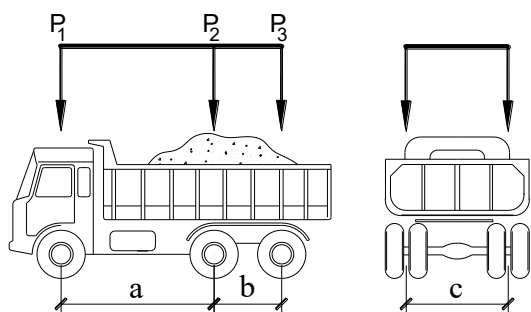


Figure 9. Test load.

If the specified vehicle is unavailable, a substitute may be used, provided it produces an equivalent measurand value.

Measurements are typically taken at key cross-sections such as mid-span for simple girders, pier tops for cantilever girders, and other critical points where structural changes occur. the loading scheme must be carefully designed to generate the most unfavourable internal forces, with a centred load diagram being mandatory. Depending on structural behaviour, eccentric loading upstream or downstream may also be applied. During load testing, each scheme includes one trial run and three official measurements in accordance with bridge testing procedures.

In this diagram, 9 cars are arranged in 3 rows with 3 cars in each row, with the middle axle of the second row positioned in the cross-section of the 0.4*l* border span and the distance from the rear axle of the front row to the front axle of the rear car is 8 m.

In the horizontal direction of the bridge, vehicles can be arranged in two options:

- arrange vehicles according to the correct centre diagram (load diagram Fig. 10b);
- arrange vehicles according to the eccentric diagram (load diagram Fig. 10c).

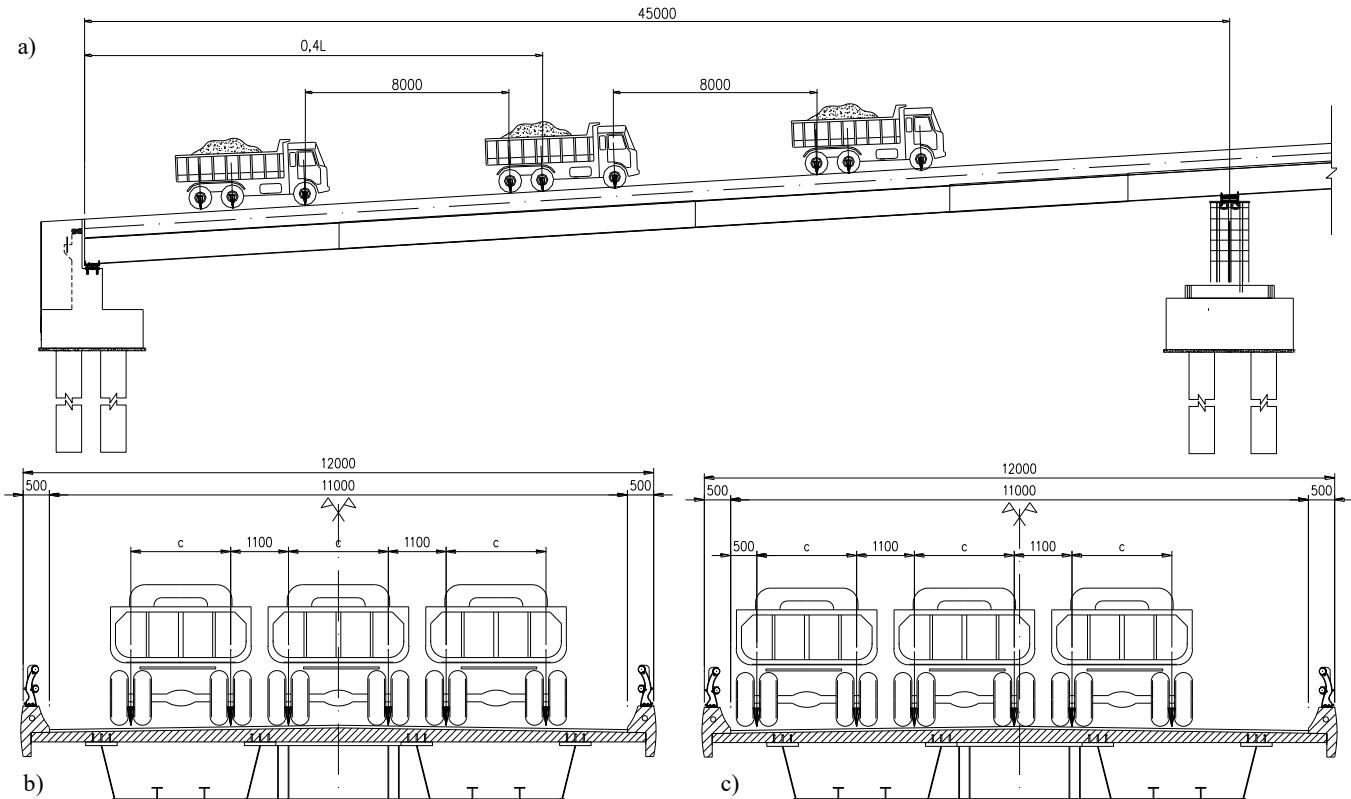


Figure 10. Load diagram: a) loading longitudinally on the bridge; b) load the bridge horizontally by the right centre diagram c) loading horizontal bridge by eccentric diagram.



Figure 11. Loading the O Dong Mac bridge: a) b) installing steel box girder stress measuring device; c) arranging the load on the bridge.

## RESULTS

Results from the Midas civil modelling are shown in Fig. 12.

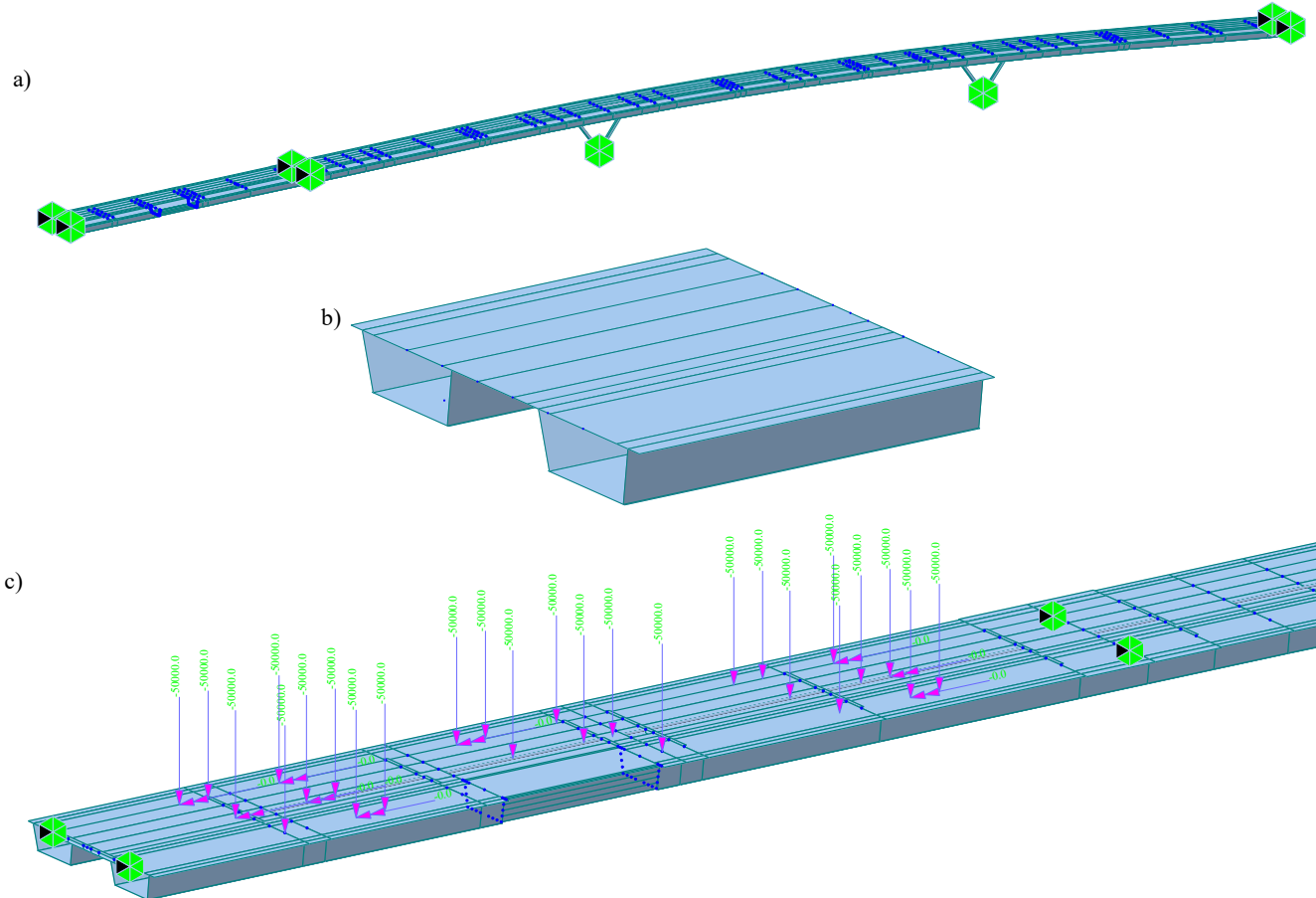


Figure 12. Bridge construction model: a) overall model; b) cross-section model of the bridge; c) load model on the bridge.

The bending moment diagram is shown in Fig. 13.

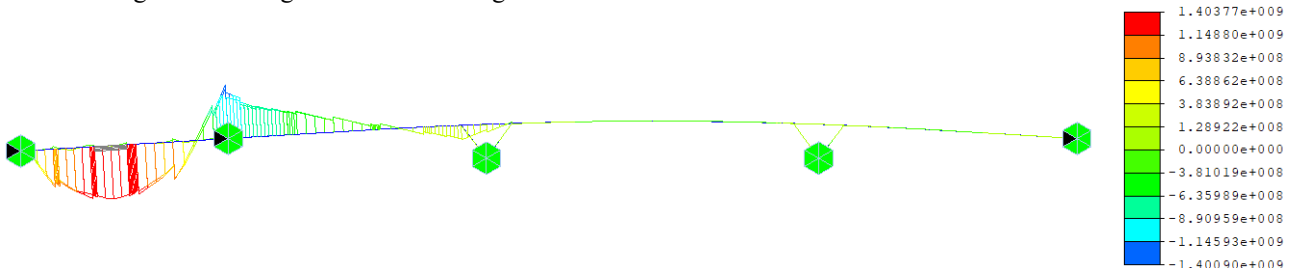


Figure 13. Bending moment diagram.

The displacement diagram is shown in Figure 14.

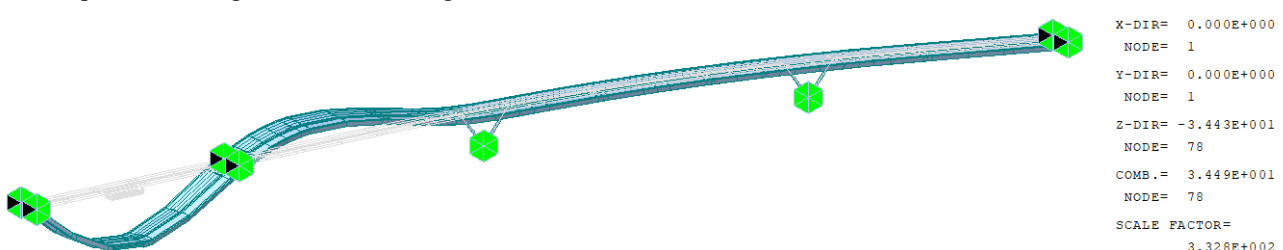


Figure 14. Displacement diagram.

Tensile and compressive stress on steel box girder when using beam element type are shown in Figs. 15, 16.

The stress diagram of steel box section when selecting the plate element is shown in Fig. 17.

Consider the strain and stress in section 1-1 (0.4l from beam end) and loading at the right centre. The experimental results obtained are given in Table 1.

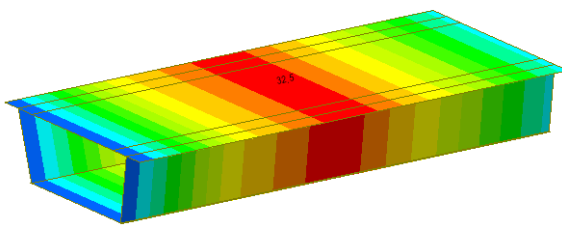


Figure 15. Tensile stress when using beam element type.

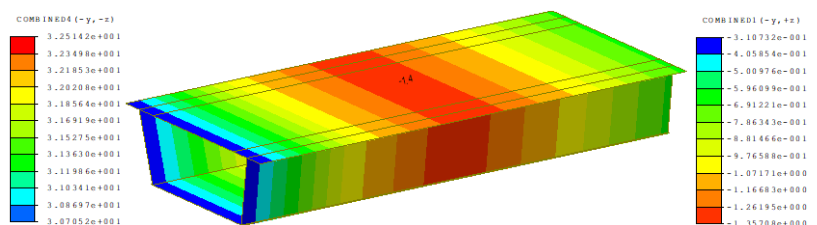


Figure 16. Compression stress when using beam element type.

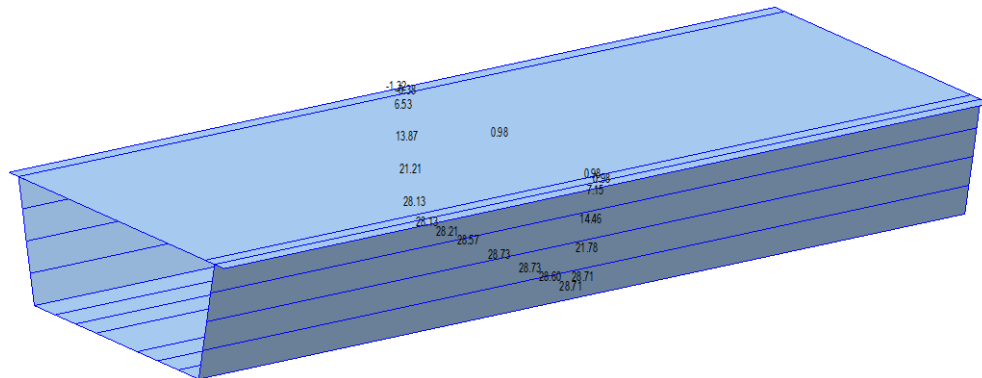


Figure 17. Stress diagram when using plate element type.

Table 1. Stress measurement results at section 1-1.

Diag.	Measuring point	Relative deformation, $\varepsilon \times 10^{-5}$				Stress (MPa)	Note
		1 <sup>st</sup> measurement ( $\varepsilon_1$ )	2 <sup>nd</sup> measurement ( $\varepsilon_2$ )	3 <sup>rd</sup> measurement ( $\varepsilon_3$ )	$(\varepsilon_1 + \varepsilon_2 + \varepsilon_3)/3$		
I <sub>a</sub>	T <sub>11</sub>	-0.25	-0.375	-0.25	-0.292	-0.583	
	T <sub>12</sub>	13.125	12.5	13.75	13.125	26.250	
	T <sub>13</sub>	13.25	12.75	12.50	12.833	25.667	
	T <sub>14</sub>	-0.375	-0.50	0	-0.432	-0.875	remove value 0
	T <sub>15</sub>	-0.25	-0.25	-0.50	-0.333	-0.667	
	T <sub>16</sub>	12.75	12.875	12.75	12.792	25.583	
	T <sub>17</sub>	12.50	12.50	13.125	12.708	25.417	
	T <sub>18</sub>	-0.25	-0.50	-0.50	-0.417	-0.833	

Results of measuring displacement at section 1-1 (0.41 from beam end) and loading at the right centre are shown in Table 2.

Comparison of stress and displacement results between experiment and numerical model is shown in Tables 3 and 4.

Table 2. Displacement measurement results at section 1-1.

Diag.	Measuring point	Number of measuring lines				Displacement (mm)	Note
		1 <sup>st</sup> measurement (f <sub>1</sub> )	2 <sup>nd</sup> measurement (f <sub>2</sub> )	3 <sup>rd</sup> measurement (f <sub>3</sub> )	(f <sub>1</sub> + f <sub>2</sub> + f <sub>3</sub> )/3		
I <sub>a</sub>	V <sub>11</sub>	1669.50	1644	1693	1668.83	16.688	
	V <sub>12</sub>	1710	1698.50	1708	1705.50	17.055	
	V <sub>13</sub>	1694	1717	1722.50	1711.17	17.112	
	V <sub>14</sub>	1686	1683.50	975	1684.75	16.848	remove value 975

Table 3. Compared stress results between experiment and numerical model.

Node point on model	Measuring point on the bridge	Experimental results (MPa)	Numerical model (MPa)			
			Element beam	Error (%)	Element plate	Error (%)
72	T1	-0.583	-1.4	140.14	-0.55	-5.66
30	T2	26.25	32.5	23.81	28.1	7.05
9	T3	25.67	32.3	25.83	28.7	11.80
51	T4	-0.833	-1.7	104.08	-0.56	-32.77

Table 4. Compared displacement results between experiment and numerical model.

Node point on model	Measuring point on the bridge	Experimental results (mm)	Numerical model	
			Element beam	Element plate
30	V1	17.055	34.4	32.5
9	V2	17.112	34.4	32.5

When the stress results from the finite element model are compared to experimental measurement results, it is discov-

ered that results from the numerical model with the plate element taking into account the warping effect of the section

give results, are very close to stress measurement results. The difference between the numerical model and the experiment is approximately 7 to 11 %. However, when the beam element is selected in the numerical model, the obtained stress results differ significantly from experimental results.

Displacement measurement results between experiment and the numerical model are significantly different. The numerical model and experiment yield different results which can be explained as follows: when calculating the numerical model, the bonding and material conditions are simplified. There are also errors in experimental measurements.

## CONCLUSIONS

Based on the obtained research results, the following conclusions can be drawn.

- The warping effect has a significant impact on the internal force and displacement of a steel box girder span structure.
- When using the plate element, a numerical model of the bridge structure that accounts for warping produces accurate results. When using plate elements, the error between numerical model results and experimental results ranges from 7 to 11 %.

## REFERENCES

1. Xiao, Q., Huang, H., Tang, C. (2023), *Quantitative analysis of the importance and correlation of urban bridges and roads in the study of road network vulnerability*, Adv. Bridge Eng. 4: 18. doi: 10.1186/s43251-023-00096-z
2. Liu, Z., Zhang, X., Chen, T., et al. (2022), *Aerodynamic loads and bridge responses under train passage: case study of an overpass steel box-girder cable-stayed bridge*, Adv. Bridge Eng. 3: 1. doi: 10.1186/s43251-021-00051-w
3. Agarwal, P., Pal, P., Mehta, P.K. (2023), *Finite element analysis of reinforced concrete curved box-girder bridges*, Adv. Bridge Eng. 4: 1. doi: 10.1186/s43251-023-00080-7
4. Helwig, T., Yura, J., Herman, R., et al. (2007), *Design guidelines for steel trapezoidal box girder systems*, Tech. Report (09/01/01 - 08/31/04), Rep. No. FHWA/TX-07/0-4307-1, Texas Dept. of Transportation, 84 p.
5. Begum, Z., *Analysis and behavior investigations of box girder bridges*, Master thesis, Dept. of Civil and Environmental Eng., University of Maryland, College Park, 2010.
6. TCVN 11823:2017 Specification for highway bridge design in Vietnam. (Vietnamese)
7. Tran, D.-B. (2024), *Non-uniform torsion behavior of thin-walled beams according to the finite element method*, Slovak J Civ. Eng. 32(3): 1-12. doi: 10.2478/sjce-2024-0014
8. Pavazza, R., Matoković, A., Vukasović, M. (2020), *A theory of torsion of thin-walled beams of arbitrary open sections with influence of shear*, Mech. Based Des. Struct. Mach. 50(1): 206-241. doi: 10.1080/15397734.2020.1714449
9. Kollrunner, C.F., Basler, K., *Torsion in Structures: An Engineering Approach*, 1<sup>st</sup> Ed., Springer Berlin, Heidelberg, 1969. doi: 10.1007/978-3-662-22557-8
10. Mbachu, V.C., Osadebe, N.N. (2013), *Torsional response of continuous thin walled box girder structures*, J Eng. Res. Appl. 3(6): 1117-1122.
11. Heinrich, S.M. (1996), *Membrane analogy for Saint-Venant torsion: new results*, J Eng. Mech. 122(11). doi: 10.1061/(ASCE)0733-9399(1996)122:11(1110)
12. Fan, Z., Helwig, T.A. (2002), *Distortional loads and brace forces in steel box girders*, J Struct. Eng. 128(6): 710-718. doi: 10.1061/(ASCE)0733-9445(2002)128:6(710)
13. Khalil, A.H.H. (2001), *Effect of warping and distortion on box girders*, In: 9<sup>th</sup> Int. Conf. on Structural and Geotechnical Eng., Ain Shams University, Cairo, Egypt, 2001.
14. Wang, Z. (2023), *Optimization methods for the distortion of thin-walled box girders and investigation of distortion effects*, Sci. Rep. 13(1): 19166. doi: 10.1038/s41598-023-46478-1
15. Bian, M., Zhang, X., Li, J., et al. (2024), *An improved shear lag analysis method for composite box girders with corrugated steel webs*, Buildings, 14(12): 4087. doi: 10.3390/buildings14124087
16. Zhu, Y.-J., Wang, J.-J., Nie, X., et al. (2020), *Structural performance of slabs in composite box girder considering compressive membrane action*, Eng. Struct. 212: 110457. doi: 10.1016/j.engstruct.2020.110457
17. Vu, Q.V., Thai, D.K., Kim, S.E. (2018), *Effect of intermediate diaphragms on the load-carrying capacity of steel-concrete composite box girder bridges*, Thin Wall Struct. 122: 230-241. doi: 10.1016/j.tws.2017.10.024
18. Huang, H., Xu, X., Ma, H., et al. (2025), *Construction control technology and monitoring analysis of walking incremental launching construction of small-curvature steel box girder bridges across expressways*, Appl. Sci. 15(2): 585. doi: 10.3390/app15020585
19. El-masry, A.A., Rabou, S.M.A., Ghannam, M. (2024), *Design resistance strengths of composite steel box girder bridge using different codes*, Innov. Infrastruct. Solut. 9: 369. doi: 10.1007/s41062-024-01637-9
20. Abbas, H.M. (2020), *Optimization of steel trapezoidal box-girders using genetic algorithm*, IOP Conf. Ser.: Mater. Sci. Eng. 928: 022023. doi: 10.1088/1757-899X/928/2/022023

© 2025 The Author. Structural Integrity and Life, Published by DIVK (The Society for Structural Integrity and Life 'Prof. Dr Stojan Sedmak') (<http://divk.inovacionicentar.rs/ivk/home.html>). This is an open access article distributed under the terms and conditions of the [Creative Commons Attribution-NonCommercial-NoDerivatives 4.0 International License](http://creativecommons.org/licenses/by-nc-nd/4.0/)